Chapter 3

BEAMS AND LENSES

An axially symmetric electric or magnetic field can be used to focus a beam of electrons much as a light lens focuses visible rays. Figure 3-1 illustrates the focusing action of a converging light lens. Rays that pass through the lens close to the axis and in directions nearly parallel to the

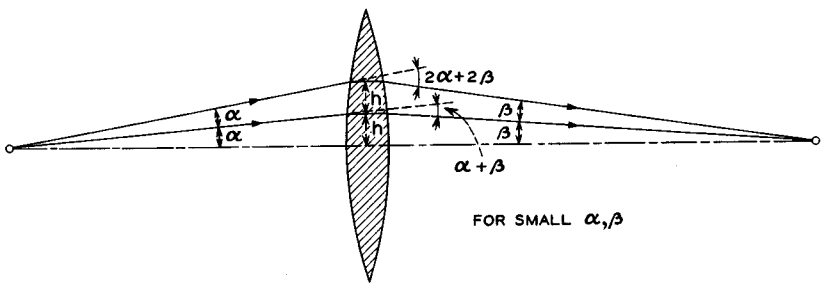

FIG. 3.1 The focusing action of a converging light lens on rays which are close to the axis and nearly parallel to the axis.

axis are given a deflection which is proportional to the distance of the rays from the axis.

An axially symmetric electric or magnetic field, or a combination of the two, acts in a similar manner on the trajectories of electrons traveling through the field. Electrons that enter the field along paths close to the axis and nearly parallel to the axis experience a radial force which is proportional to the distance of the electrons from the axis. The electron trajectories therefore are deflected in proportion to their distance from the axis, and the axially symmetric field acts as a lens. Figures 3-2(a) and 3-2(b) illustrate an electric electron lens and a magnetic electron lens, respectively.

A considerable parallelism exists between the geometric relations that govern the paths of light rays through a light lens and those that govern the trajectories of electrons through an electron lens. However, it will be useful to note several important differences between the two kinds of lenses.

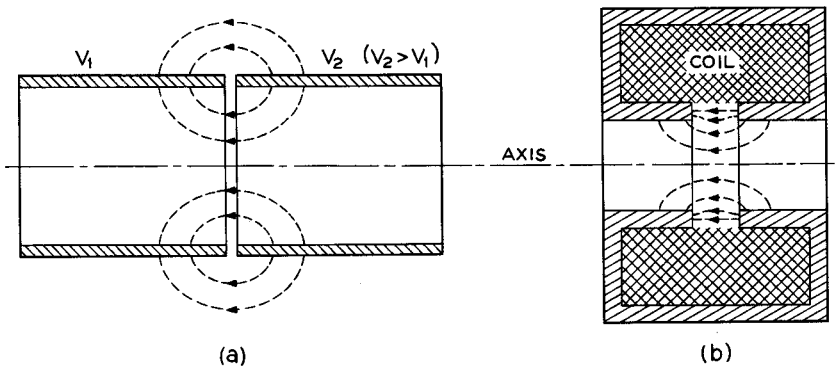

FIG. 3.2 An electric electron lens and a magnetic electron lens.

In the first place, the boundaries of a light lens are usually well defined, whereas an electron lens between field-free regions has no well-defined boundaries, since the field approaches zero asymptotically at the ends of the lens. Rays passing through a light lens, such as that illustrated in Figure 3-1, suffer abrupt changes in direction in passing between the different media that make up the lens, but the electron trajectories in an electron lens change only in a continuous manner. The electron lens has greater versatility than a light lens in that its strength can be varied merely by changing the field intensity. However, we shall find that a charge-free region of axially symmetric electric or magnetic field can act only as a converging lens on a beam of electrons whose path begins and ends in regions of zero field. In this respect there is no counterpart to the diverging lens of light optics. Furthermore, aberrations in electron lenses are generally greater than in light lenses, and correcting for the aberrations is much more difficult. Finally, a magnetic electron lens causes a rotation of the image about the axis of the lens, and there is no counterpart to this in light optics.

It will be convenient to make use of several simplifications in notation in expressing the equations we shall use in this chapter. A single dot over a variable will be used to indicate the first derivative with respect to time, and a double dot will indicate the second derivative with respect to time. Thus $\dot{r} = dr/dt$, and $\ddot{r} = d^2r/dt^2$. Similarly $r' = dr/dz$, and $r'' = d^2r/dz^2$,

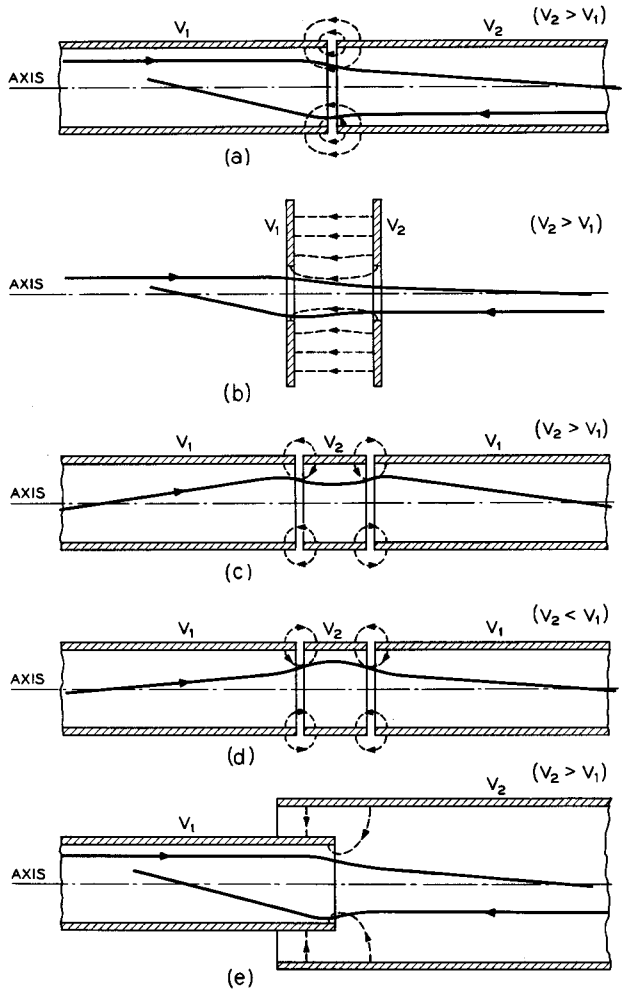

FIG. 3.1-1 Several electric electron lenses. Approximate shapes of trajectories of electrons passing through the lenses are shown by the solid lines.

where z is the axial coordinate. The ratio e/m appears frequently in the equations, and we shall denote it by η.

3.1 Electric Lenses

Figure 3.1-1 illustrates several types of electric lenses. The approximate shapes of trajectories of electrons passing through the lenses are shown in

the figure. The lens shown in Figure 3.1-1(a) is formed by two coaxial cylinders of equal radius, the one at the right being at higher potential than the one at the left. An arrow on the upper trajectory indicates that it is the trajectory of an electron which passes through the lens from left to right. To the left of the gap the electron experiences a radial force tending to deflect it toward the axis, whereas to the right of the gap the radial force is directed away from the axis. However, since the electron is further from the axis to the left of the gap, and since the radial component of the field increases with distance from the axis, the inward force to the left of the gap is stronger. Furthermore, the electron travels more slowly to the left of the gap because it is in a region of lower potential. Consequently, the trajectory receives a net deflection toward the axis, and some distance to the right of the lens the electron crosses the axis.

The lower trajectory shown in Figure 3.1-1(a) is that of an electron which travels from right to left. As the electron enters the field, it is at first deflected away from the axis. However, after passing the gap, the electron travels more slowly, and since it is further from the axis, it experiences a relatively strong inward force. The electron, therefore, receives a net deflection toward the axis in passing through the lens.

Similar reasoning applies to the other electron trajectories shown in Figure 3.1-1. Each trajectory is reversible in the sense that an electron emerging from the lens would follow the same path back through the lens if its direction of travel were reversed without changing the magnitude of its velocity. Clearly, for a given potential difference between the electrodes, the faster an electron is traveling at the time it passes through a lens, the smaller the angle through which it will be deflected.

A particularly interesting lens is that illustrated in Figures 3.1-1(c) and 3.1-1(d). The lens focuses an electron beam for either $V_2 > V_1$ or $V_2 < V_1$. By holding V_1 constant and varying V_2, the stength of the lens can be varied without changing the electron velocity on either side of the lens. Such a lens is used in many cathode-ray tubes to focus the electron beam. It is often called an einzel lens. The German word "einzel" means "single" and is used in this case to imply that the potential and the electron velocity are the same on either side of the lens.

Let us consider the radial forces acting on an electron in an axially symmetric electric field. In Appendix V it is shown that the potential at radius r from the axis of an axially symmetric potential distribution is given in terms of the potential along the axis by

$$V(z,r) = V(z,0) - \frac{r^2}{4}V''(z,0) + \frac{r^4}{64}V''''(z,0) - \ldots \qquad (3.1\text{-}1)$$

where $V(z,0)$ is the potential along the axis, and the primes indicate differentiation with respect to z. By means of Equation (3.1-1) the potential

at all points in an axially symmetric potential distribution can be described in terms of the potential on the axis. For regions close to the axis we can neglect all but the first two terms of this expression, so that

$$V(z,r) = V(z,0) - \frac{r^2}{4}V''(z,0) \tag{3.1-2}$$

and the radial gradient of potential is given by

$$\frac{\partial V(z,r)}{\partial r} = -\frac{r}{2}V''(z,0) \tag{3.1-3}$$

Since the radial force acting on an electron is given by $-eE_r = e(\partial V/\partial r)$, it follows that for small r the radial force is proportional to the distance of the electron from the axis. If the electron is traveling nearly parallel to the axis, its trajectory is deflected by an amount proportional to the distance of the trajectory from the axis. This therefore explains the lens action of an axially symmetric electric field.

Figure 3.1-2 shows a two-cylinder electron lens in which the spacing between the cylinders is small compared with their radii. An expression[1]

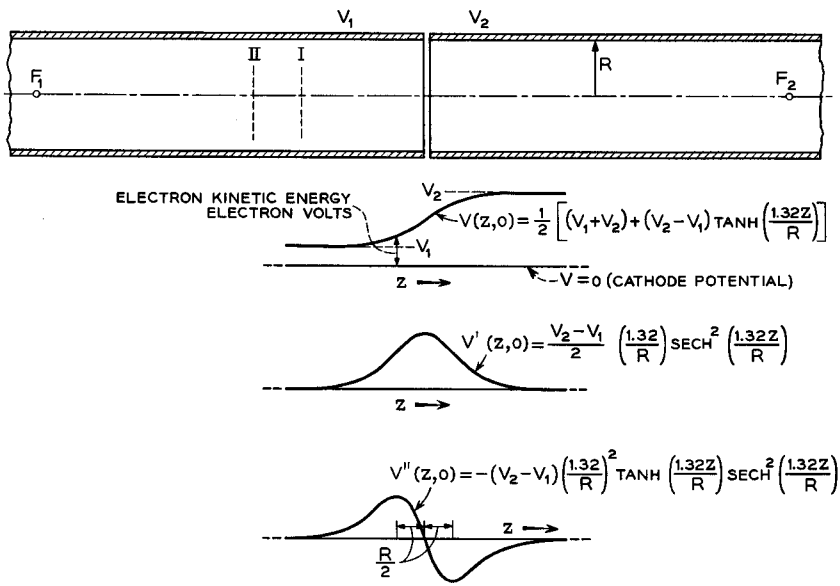

FIG. 3.1-2 A two-cylinder electric lens. The axial potential $V(z,0)$ and its first and second derivatives are shown below the lens. The positions of the principal planes and the focal points for $V_2 = 4V_1$ are indicated (see Figure 3.1-4).

[1]Reference 3.1.

for the potential along the axis $V(z,0)$ is plotted in the figure together with plots of $V'(z,0)$ and $V''(z,0)$. The potential $V(z,0)$ varies only slightly with changes in spacing between the cylinders, provided the spacing remains small compared with the radii of the cylinders. From the foregoing discussion it is evident that the radial force on an off-axis electron is proportional to the product of the distance of the electron from the axis and $V''(z,0)$. To the left of the mid-point between the cylinders the radial force is directed toward the axis, and for a given value of r it reaches a maximum $R/2$ to the left of the mid-point, where R is the radius of the cylinders. To the right of the mid-point the radial force is outward, and for a given value of r it reaches a maximum $R/2$ to the right of the mid-point.

The equation describing the trajectory of an electron that travels nearly parallel to the axis of an axially symmetric electric field and at a small distance r from the axis is known as the paraxial-ray equation. It will be helpful to derive this equation, since we shall use it in later discussion. From Equation (3.1-3), we can express the radial force acting on an electron as

$$m\ddot{r} = e\frac{\partial V(z,r)}{\partial r} = -\frac{er}{2}V''(z,0) \tag{3.1-4}$$

Now

$$\dot{r} = r'\dot{z} \tag{3.1-5}$$

and

$$\ddot{r} = r''(\dot{z})^2 + r'\ddot{z} \tag{3.1-6}$$

If the electron trajectory is nearly parallel to the axis, $\dot{z}$ will be approximately equal to the total velocity of the electron, and $(\dot{z})^2$ can be equated to $2\eta V(z,r)$, where $\eta = e/m$, *and* $V(z,r)$ *is measured relative to cathode potential.* The quantity $\ddot{z}$ on the right-hand side of Equation (3.1-6) is equal to the instantaneous acceleration of the electron in the z direction, or $\eta V'(z,r)$. Furthermore, $V(z,r) \approx V(z,0)$ and $V'(z,r) \approx V'(z,0)$, so that Equation (3.1-6) can be rewritten as

$$\ddot{r} = 2\eta V(z,0)r'' + \eta V'(z,0)r' \tag{3.1-7}$$

Combining this with Equation (3.1-4), we obtain

$$r'' + \frac{V'(z,0)}{2V(z,0)}r' + \frac{V''(z,0)}{4V(z,0)}r = 0 \tag{3.1-8}$$

This is the paraxial-ray equation which we set out to derive. Several important conclusions can be drawn from it:

1. If $r_1(z)$ and $r_2(z)$ are two independent solutions of the equation, then $ar_1(z) + br_2(z)$ is also a solution of the equation, and, in fact, any solution $r_3(z)$ can be expressed in the form $r_3(z) = ar_1(z) + br_2(z)$.

2. Since the equation is homogeneous in V, increasing the electrode potentials in the same proportion does not change the shape of the trajectory through the lens. Furthermore, the equation is independent of e and m, so that an electron or a negatively charged ion accelerated through the same potential rise and entering the lens along the same trajectory would follow the same path through the lens.

Equation (3.1-8) can be expressed in a second useful form by substituting

$$r = SV^{-1/4} \tag{3.1-9}$$

where $V = V(z,0)$. This leads to

$$S'' + \frac{3}{16}\left(\frac{V'}{V}\right)^2 S = 0 \tag{3.1-10}$$

Let us integrate Equation (3.1-10) along the axis of an axially symmetric field from one region of zero field to another. We obtain

$$S_2' - S_1' = -\frac{3}{16}\int_{z_1}^{z_2}\left(\frac{V'}{V}\right)^2 S\,dz \tag{3.1-11}$$

where z_1 and z_2 are the z coordinates of two points on the axis on opposite sides of the lens and at which the potential gradient is zero. The point z_1 is assumed to be on the initial side of the lens, and the point z_2 is on the final side. Since the integrand on the right-hand side is always greater than zero, it follows that

$$S_2' - S_1' < 0 \tag{3.1-12}$$

Now $S = rV^{1/4}$, and $S' = r'V^{1/4} + rV'/4V^{3/4}$. Consider an electron which approaches the lens along a path that is parallel to the axis but displaced from it. For such an electron

$$S_1' = \left| r'V^{1/4} + rV'/4V^{3/4} \right|_{z_1} = 0$$

since $r' = V' = 0$ at $z = z_1$. It follows from Equation (3.1-12) that $S_2' < 0$. However, at $z = z_2$, $V' = 0$, so that $r' < 0$ at $z = z_2$. Thus the path of the electron is bent toward the axis by the field, and we must conclude that *all charge-free regions of axially symmetric electric field between field-free regions act as converging lenses.*

If an electron approaches a lens along a path that is parallel to the axis but displaced from it, the electron emerges from the lens as though it were deflected at a plane which generally is not at the geometrical center of the lens. This effect is illustrated in Figure 3.1-3 for several trajectories passing through an axially symmetric field at different distances from the axis. The plane at which the trajectories appear to have been deflected is called a *principal plane,* and the point where the electrons ultimately cross the

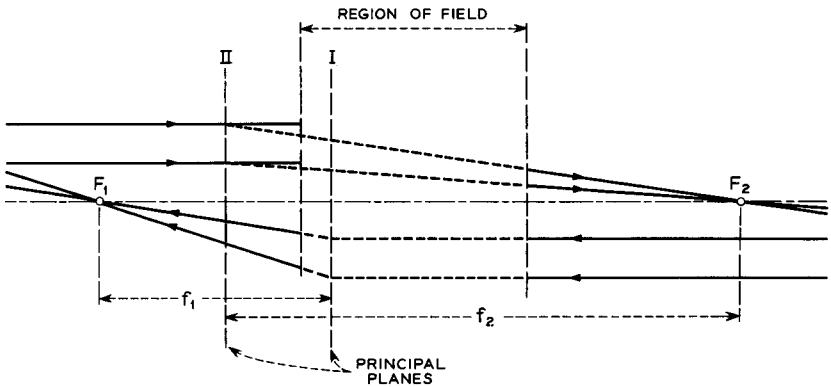

FIG. 3.1-3 The principal planes, the focal lengths, and the focal points of a lens.

axis is called a *focal point.* The distance from the principal plane to the focal point is called the *focal length.* There are two principal planes I and II, two focal points F_1 and F_2, and two focal lengths f_1 and f_2, one of each associated with electrons moving in either direction through the lens. If the electrodes and their potentials are symmetrical about the geometrical mid-point of the lens, as in the case of the einzel lens shown in Figures 3.1-1(c) and 3.1-1(d), the focal points and principal planes are also symmetrically located about the mid-point. However, in the case of the lens shown in Figure 3.1-2, where the potentials are not the same on either side of the geometrical mid-point, the principal planes are displaced toward the low-voltage side of the lens, and the focal lengths are not equal. The location of the principal planes and focal points is shown in Figure 3.1-2 for the case in which the potential of the right-hand cylinder is four times that of the left-hand cylinder.

Mathematical expressions for the potential $V(z,0)$ along the axis of a lens are available for only a few electrode configurations, one example being the two-cylinder lens of Figure 3.1-2. Goddard[2] has used the expression for $V(z,0)$ given in Figure 3.1-2 to obtain solutions of the paraxial-ray equation for the case of electrons which approach the lens along paths that are parallel to the axis but displaced from it. In this way the positions of the principal planes and the focal lengths of the lens were determined as functions of V_2/V_1. Figure 3.1-4 shows plots of the focal lengths f_1 and f_2 and the distances x_1 and x_2 from the mid-point of the lens to the principal planes for a range of values of V_2/V_1. The location of the principal planes is found to remain nearly constant for V_2/V_1 greater than about 4.

[2]Reference 3.2.

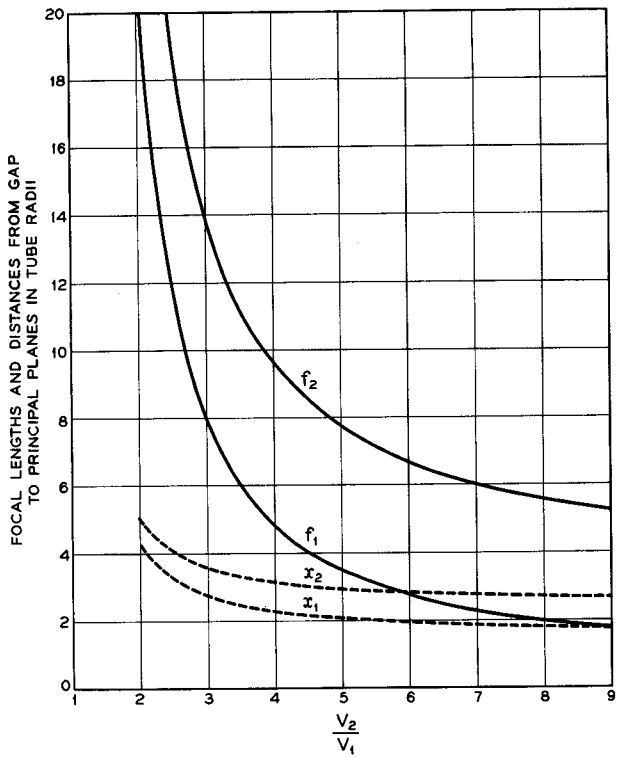

FIG. 3.1-4 The focal lengths f_1 and f_2 for a two-cylinder lens, such as that shown in Figure 3.1-2, as a function of the ratio of the potentials applied to the cylinders. The potentials V_1 and V_2 are measured relative to that of the cathode from which the electrons are emitted. The distances x_1 and x_2 from the gap between the cylinders to the principal planes are also plotted in the figure. (From L. S. Goddard, *Proc. Cambridge Phil. Soc.* **42**, 106, 1946)

In general, expressions for $V(z,0)$ are very complicated, so that an explicit solution of the paraxial ray equation is difficult, if not impossible, to obtain. Furthermore, for many electrode configurations an expression for $V(z,0)$ is not available. When there is no expression for $V(z,0)$, the electrode configuration can be simulated in an apparatus called an electrolytic tank,[3] and the axial potential can be measured experimentally. Approximate solutions to the paraxial-ray equation can then be obtained by breaking the field up into a number of segments in the axial direction

[3]See, for instance, Reference 3b, Figure 5.15, p. 67.

and estimating the path of an electron across each segment.[4] In a few specific electron lenses, data concerning the locations of the principal planes and focal lengths have been obtained by direct measurement of the focusing action of the lenses upon electron beams passing through them. Such data are given in Reference 3.5 and in Reference 3e, pp. 369-373.

In Appendix VI the following relations between the object position, the image position, and the focal lengths of an electron lens are derived:

$$\frac{f_1}{u} + \frac{f_2}{v} = 1 \tag{3.1-13}$$

$$\text{magnification} = \frac{\text{image size}}{\text{object size}} = \frac{f_1}{f_2}\frac{v}{u} \tag{3.1-14}$$

and

$$\frac{f_2}{f_1} = \left(\frac{V_2}{V_1}\right)^{1/2} \tag{3.1-15}$$

where the object is located u units to the left of the first focal plane and the image is located v units to the right of the second focal plane. The region to the left of the lens is at potential V_1 with respect to the cathode, and the region to the right of the lens is at potential V_2. From Equation (3.1-15) we see that for the two-cylinder lens shown in Figure 3.1-2 the focal length f_2 is twice f_1, when $V_2 = 4V_1$.

In a cathode-ray tube the electron gun directs the beam to a "crossover," and a lens beyond the crossover forms an image of the crossover at the screen of the tube. Using Equations (3.1-13) and (3.1-14), the position of the image and its magnification can be related to the focal lengths of the lens and the position of the crossover.

The concepts of principal planes, of focal points, and of focal lengths have been adopted from light optics, where they are used to describe the paths of light rays through lenses. The arguments that are employed in Appendix VI to derive Equations (3.1-13) and (3.1-14) apply equally well to a light lens, and, in fact, Equations (3.1-13) and (3.1-14) are of principal importance in work with light lenses. It can be shown that the square root of electric potential in the case of an electron lens is analogous to index of refraction in light optics. For a light lens at the surface between two media of different indices of refraction, the ratio of the focal lengths is given by $f_2/f_1 = n_2/n_1$, where n_1 and n_2 are, respectively, the refractive indices of the media in which the focal points F_1 and F_2 are located. The two-cylinder lens shown in Figure 3.1-2 is therefore analogous to a light lens

[4]Methods for making such computations are discussed in: Reference 3.3; Reference 3.4; Reference 3a, Chapter III; Reference 3b, p. 101; Reference 3e, p. 360.

at the boundary between two media of different refractive indices, whereas the einzel lens is analogous to a light lens surrounded by a medium of the same index of refraction.

3.2 Magnetic Lenses

Figure 3.2-1 shows a magnetic lens that is formed by a cylindrical permanent magnet and two re-entrant pole pieces. Since the magnetic potential outside the magnetic material satisfies Laplace's Equation, the off-axis magnetic potential can be expressed in terms of the potential on the axis using Equation (3.1-1), where $V(z,0)$ is replaced by $\psi(z,0)$, the magnetic potential on the axis. The magnetic flux density **B** in a region of free space is proportional to the gradient of magnetic potential, and it follows from the magnetic equivalent of Equation (3.1-3) that the radial component of **B** is directly proportional to r for small r. The z component of **B**, on the other hand, is nearly constant with r for small r, since the equipotential surfaces are normal to the axis at the points where they cross the axis.

Consider an electron that enters the lens shown in Figure 3.2-1 from the left along a path that is initially parallel to the axis but displaced a small distance from it. To the left of the gap the radial component of **B** is directed toward the axis and, since the force acting on an electron in a magnetic field is $-e(\mathbf{u} \times \mathbf{B})$, the electron experiences a force that is directed out of the page. This gives the electron angular momentum about the axis, so that it crosses the z component of **B** as it passes through the central region of the lens. The z component of **B** deflects the electron toward the axis as it passes through the central part of the lens. Beyond the center of the lens the lines of **B** have a radial component away from the axis, and the electron loses angular velocity about the axis. We shall find that when the electron has traveled beyond the region of field, its angular velocity about the axis is reduced to zero. The electron therefore emerges from the lens with a radial component of velocity, which is directed toward the axis, and with no angular velocity. At some point beyond the lens the electron trajectory passes through the axis.

Suppose that two electrons approach the lens along paths that are parallel to the axis and lying in a plane containing the axis. One path is twice as far from the axis as the second, and the radial distance from the axis to each of the paths is small. As the electrons enter the magnetic field, the radial component of **B** encountered by the outer electron is twice that encountered by the inner electron, so that the outer electron acquires twice as much velocity in the θ direction. The *angular* velocity of the two electrons about the axis is therefore the same, and the outer electron crosses the z

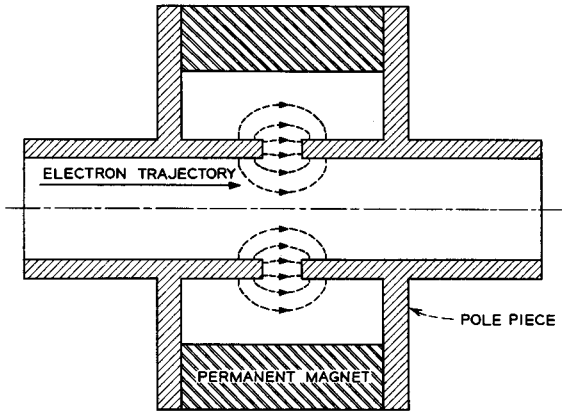

FIG. 3.2-1 A magnetic electron lens.

component of **B** with twice as much velocity and receives twice as much deflection toward the axis. Beyond the center of the lens, the outer electron again experiences twice the radial component of **B**, this time directed away from the axis, and loses twice as much velocity in the θ direction. Both electrons therefore emerge from the lens with zero angular velocity, and, since the outer electron received twice as much deflection toward the axis, both are directed toward the same point on the axis. Consequently, the trajectories to the right of the lens lie in a plane which contains the axis, but which is rotated about the axis from the plane that contained the trajectories to the left of the lens.

It will be helpful to develop two equations that describe the motion of an

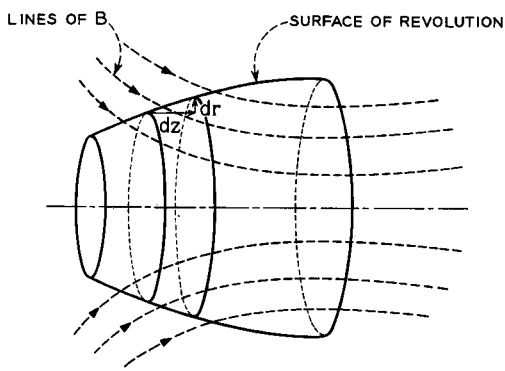

FIG. 3.2-2 A surface of revolution which contains the electron trajectory. The axis of the surface of revolution coincides with that of the field.

electron as it travels through an axially symmetric magnetic field along a path close to the axis and nearly parallel it. The electron is assumed to have zero initial angular velocity about the axis. The first equation relates the instantaneous angular velocity of the electron to the axial magnetic field, and the second describes the radial motion of the electron in passing through the field. The second equation is known as the paraxial-ray equation for magnetic fields.

Figure 3.2-2 shows a portion of a surface of revolution which contains the trajectory of an electron that enters the magnetic field along a path directed away from the axis. The axis of the surface of revolution coincides with that of the field. As the electron crosses the lines of **B**, it experiences a force in the θ direction, and from Equation (1.2-5) we can write that

$$\frac{d(r^2\dot{\theta})}{dt} = \eta r(\dot{r}B_z - \dot{z}B_r) \tag{3.2-1}$$

where $\dot{\theta} = d\theta/dt$ and $\eta = e/m$. Multiplying by dt, we obtain

$$d(r^2\dot{\theta}) = \eta r(drB_z - dzB_r) \tag{3.2-2}$$

Consider an incremental length of trajectory in which the electron advances a distance dz in the z direction and a distance dr in the r direction. The magnetic flux that crosses the portion of the surface of revolution corresponding to the axial length dz can be expressed as

$$d\Phi = 2\pi r(drB_z - dzB_r) \tag{3.2-3}$$

where $d\Phi$ is assumed to be positive if the flux within the surface of revolution increases as z increases. Combining Equation (3.2-2) with Equation (3.2-3), we obtain

$$d(r^2\dot{\theta}) = \frac{\eta}{2\pi}d\Phi \tag{3.2-4}$$

Integrating this equation along the axis from a point to the left of the lens where $\dot{\theta} = \Phi = 0$ to a point within the region of field, we obtain

$$r^2\dot{\theta} = \frac{\eta}{2\pi}\Phi \tag{3.2-5}$$

For small r, Φ is related to the axial magnetic flux density by $B_z = \Phi/\pi r^2$, so that

$$\dot{\theta} = \frac{\eta B_z}{2} \tag{3.2-6}$$

Thus the angular velocity of the electron at a given point on its trajectory is proportional to the z component of magnetic field at that point, and when the electron has traveled beyond the region of field, its angular velocity is reduced to zero.

From Equation (1.2-4), the radial force acting on the electron is given by

$$\ddot{r} - r(\dot{\theta})^2 = -\eta r\dot{\theta}B_z \tag{3.2-7}$$

Combining this with Equation (3.2-6), we obtain

$$\ddot{r} + \left(\frac{\eta B_z}{2}\right)^2 r = 0 \tag{3.2-8}$$

Now for an electron traveling nearly parallel to the axis of an axially symmetric magnetic field in a region where the electric potential is constant, Equation (3.1-7) reduces to

$$\ddot{r} = 2\eta V r'' \tag{3.2-9}$$

where V is the potential through which the electrons have been accelerated. Combining Equations (3.2-8) and (3.2-9) gives

$$r'' + \frac{\eta}{8V}B_z^2 r = 0 \tag{3.2-10}$$

This is the paraxial-ray equation for electrons traveling in an axially symmetric magnetic field when no electric fields are present. Together with Equation (3.2-6) it describes the trajectory of an electron traveling close to the axis of the field and nearly parallel to the axis. Since Equation (3.2-10) is linear, any solution of the equation can be expressed as a linear combination of any two other independent solutions.

Rewriting Equation (3.2-10) in the form

$$r'' = -\frac{\eta}{8V}B_z^2 r \tag{3.2-11}$$

we see that wherever B_z is different from zero, r'' is negative, and the trajectory is curved toward the axis. Hence *all magnetic lenses are converging.*

A "weak" lens is one for which the focal length is long compared with the region of field. Suppose that an electron approaches such a lens along a path that is initially parallel to the axis but displaced a small distance from it. Integrating Equation (3.2-11) along the axis between points on either side of the lens where the field is zero, we obtain

$$r_2' = -\frac{\eta}{8V}\int_{z_1}^{z_2} B_z^2 r dz \tag{3.2-12}$$

where z_1 and z_2 are points on the axis on opposite sides of the lens and beyond the region of field, and r_2' is the slope of the trajectory at $z = z_2$. If the focal length is long compared with the region of field, r will remain nearly constant in the region of field and can be taken outside the integral

in Equation (3.2-12). The focal length f for such a lens is then given by

$$\frac{1}{f} = -\frac{r_2'}{r} = \frac{\eta}{8V}\int_{z_1}^{z_2} B_z^2 dz \qquad (3.2\text{-}13)$$

In a magnetic lens the focal lengths f_1 and f_2 are equal; and if the magnet and pole pieces are symmetric about a central plane, the principal planes are located equal distances on either side of the central plane. In the weak lens approximation it is generally sufficient to assume that the principal planes coincide with the mid-plane of the lens.

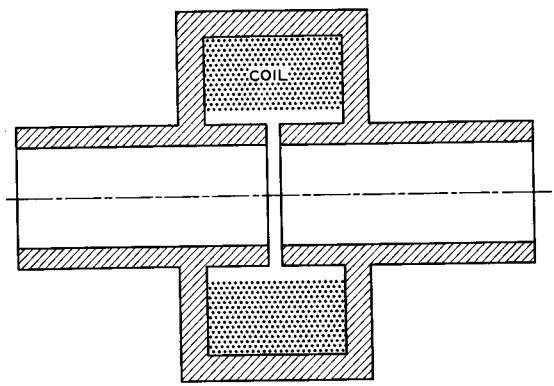

FIG. 3.2-3 An electromagnet lens.

Figure 3.2-3 shows an electromagnet lens with re-entrant pole pieces that almost touch each other. In the cylindrical region of space extending from the axis out to the pole pieces, $\int \mathbf{H}\cdot d\mathbf{l}$ around any closed path is equal to zero, and we can define a magnetic potential within the region such that the magnetic potential difference between two points is equal to $\int \mathbf{H}\cdot d\mathbf{l}$ along any path between them.[5] If the cylindrical part of the pole pieces is made of high permeability steel, so that it acts as a unipotential body, and if the spacing between the pole pieces is small compared with the inside radius of the pole pieces, a plot of magnetic potential along the axis would be of similar shape to the electric potential $V(z,0)$ plotted in Figure 3.1-2. The axial potential therefore would be proportional to tanh $(1.32z/R)$ + constant, where R is the inside radius of the pole pieces. The

[5]However, we must confine ourselves to a region that does not surround the coil, since $\int \mathbf{H}\cdot d\mathbf{l}$ along a closed path which surrounds the coil is not zero, and the magnetic potential would not be single-valued.

axial magnetic flux density would be proportional to the gradient of this and can be expressed as

$$B_z = B_o \operatorname{sech}^2\left(\frac{1.32z}{R}\right) \tag{3.2-14}$$

Substituting this expression in Equation (3.2-13), we obtain for the reciprocal of the focal length

$$\frac{1}{f} = \frac{\eta}{8V} B_o^2 \int_{z_1}^{z_2} \operatorname{sech}^4\left(\frac{1.32z}{R}\right) dz \tag{3.2-15}$$

Using the relations $\operatorname{sech}^2 z = 1 - \tanh^2 z$ and $\operatorname{sech}^2 z dz = d(\tanh z)$, we obtain

$$\begin{aligned} \frac{1}{f} &= \frac{\eta}{8V} B_o^2 \frac{R}{1.32}\left[\tanh\left(\frac{1.32z}{R}\right) - \frac{\tanh^3\left(\frac{1.32z}{R}\right)}{3}\right]_{z_1}^{z_2} \\ &= \frac{\eta}{8V} B_o^2 \frac{R}{1.32} \frac{4}{3} \approx \frac{\eta}{8V} B_o^2 R \end{aligned} \tag{3.2-16}$$

where the points z_1 and z_2 have been taken to be effectively at $-\infty$ and $+\infty$, respectively. The focal length f is therefore given by

$$f = \frac{8V}{\eta B_o^2 R} = \frac{V}{2.20 \times 10^{10} B_o^2 R} \tag{3.2-17}$$

For $V = 10^4$ volts, $B_o = 10^{-2}$ weber/meter^2, $R = 2 \times 10^{-2}$ meter (2 cm), the focal length f is 0.23 meter or 23 cm. In principle, such a lens might be used to focus the beam of a television picture tube.

If an electron trajectory on one side of a lens lies in a plane containing the axis, the trajectory after emerging from the lens will also lie in a plane containing the axis. However, the second plane is rotated about the axis from the first plane. From Equation (3.2-6) the angle of rotation between the planes is given by

$$\theta = \frac{\eta}{2} \int_{t_1}^{t_2} B_z dt = \frac{\eta}{2} \int_{z_1}^{z_2} B_z \frac{dz}{dz/dt} = \sqrt{\frac{\eta}{8V}} \int_{z_1}^{z_2} B_z dz \tag{3.2-18}$$

where t_1 and t_2 are, respectively, the times at which the z coordinate of the electron is z_1 and z_2, and where it is assumed that $\dot{z}$ is very nearly constant through the lens and is equal to $\sqrt{2\eta V}$. If B_z is in the direction of travel of the electron, θ is positive. In the case of the lens described above with $V = 10^4$ volts, $B_z = 10^{-2} \operatorname{sech}^2 (1.32z/R)$ weber/meter^2, and $R = 2 \times 10^{-2}$ meter, the angle θ is 0.45 radian, or 26 degrees.

3.3 Aberrations and Deflection Defocusing Effects

Like light lenses, electron lenses have aberrations, or imperfections in their image-forming and focusing characteristics. Figure 3.3-1 illustrates

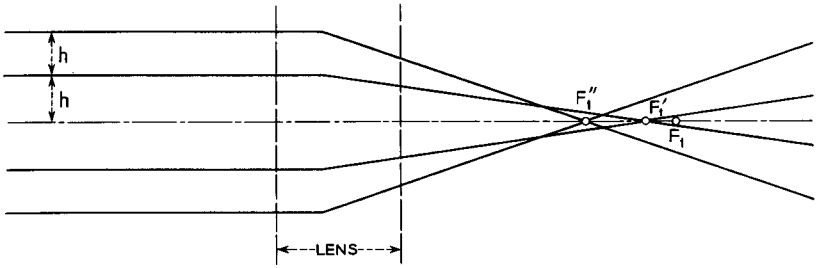

FIG. 3.3-1 Spherical aberration, or aperture defect.

one type of aberration common to all electron lenses and known as spherical aberration, or aperture defect. This is one of the most serious defects of electron lenses. Rays that pass through the lens far from the axis are focused to a different focal point than the paraxial rays. In the figure, rays that enter the lens along paths that are parallel to the axis and very close to it are focused to the point F_1. However, rays that are initially displaced

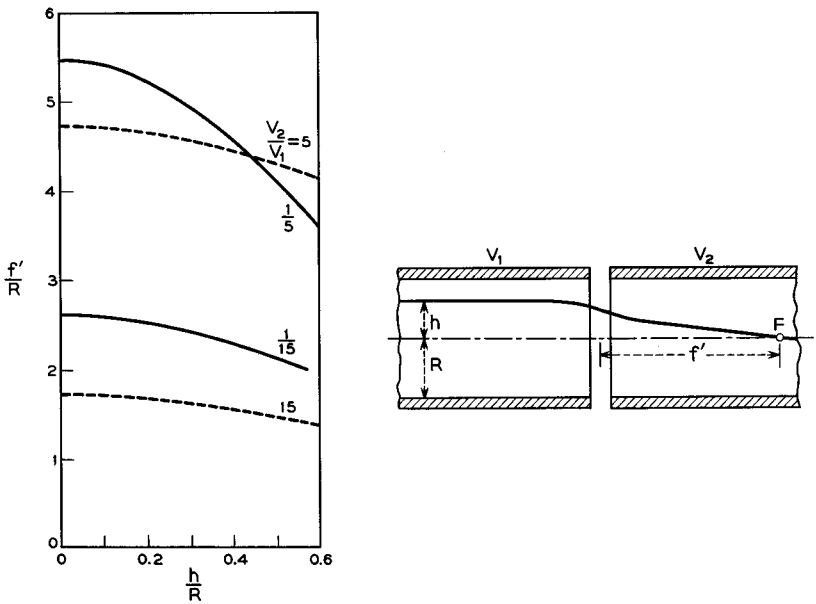

FIG. 3.3-2 Measurements of the spherical aberration in a two-cylinder electric lens. (From O. Klemperer, *Electron Optics*, 2nd Ed., Cambridge University Press, 1953)

an appreciable distance h from the axis are focused to the point F_1', and rays that are initially displaced a distance $2h$ from the axis are focused to the point F_1''. In electron lenses the focal point generally moves closer to the lens for rays that are further from the axis. The effect can be accounted for if the theory presented in Sections 3.1 and 3.2 is extended to include higher-order terms in the expressions for the off-axis fields, and if the angles through which the electron trajectories are deflected are no longer assumed to be small.

Figure 3.3-2 shows experimental data concerning the spherical aberration in a two-cylinder electron lens. Rays that approach the lens along paths that are parallel to the axis and displaced a distance h from it are deflected so that they cross the axis a distance f' from the geometrical midpoint of the lens. For a given semi-aperture h and focal length, the spherical aberration is evidently less when the electrons are accelerated in passing through the lens than when they are decelerated. To a first approximation, the axial displacement of the focal point is proportional to the square of the lens semi-aperture h. Magnetic lenses are generally found to have less spherical aberration than electric lenses of comparable focal length.

Suppose that in Figure 3.3-1 a screen were placed perpendicular to the axis at F_1. If the semi-aperture of the lens were $2h$, the rays would strike the screen over a small circular area. Moving the screen closer to the lens would at first cause the diameter of the circular area to decrease and later to increase, the condition of best focus being that corresponding to minimum diameter of the spot on the screen. The circular spot on the screen at best focus is called the circle of least confusion, as in light optics. As the semi-aperture of the lens is decreased, the diameter of the circle of least confusion decreases, and its axial position approaches the paraxial-ray focal point F_1.

A second type of aberration, known as chromatic aberration, is caused by the finite distribution of electron velocities in the beam. The faster electrons in the beam are deflected less by the lens than the slower ones. Additional types of aberrations are encountered when an electron lens of large aperture forms an image of an electron source of appreciable size. Some of these aberrations have counterparts in light optics and are identified with the same names as those used in light optics. They include coma, field curvature, astigmatism, and distortion. Magnetic lenses introduce still other aberrations associated with the rotation of the image. Factors contributing to the various types of aberrations encountered in electron optics are summarized below:

1. Higher-order components in the expressions for the off-axis fields together with geometrical factors relating to the large lens aperture and large deflection angles.

2. The distribution of electron velocities (which leads to chromatic aberration).

3. Space-charge effects in which the electrons are deflected by the electric field associated with the beam itself.

4. Mechanical imperfections in the alignment or shape of the electrodes or pole pieces.

5. In the case of magnetic lenses, inhomogeneities in the magnetic material.

Although much can be done to minimize inherent aberrations in light lenses by causing the geometrical and physical properties of the lens to change with radial distance from the axis, similar corrections in electron lenses are much harder to achieve, since the off-axis fields are directly related to the axial field. Consequently, the resolution that can be achieved with a good electron lens is far less than can be achieved with a good light lens.

Changes in beam shape and focusing also occur when a beam is deflected. Figure 3.3-3 shows an electron beam that passes through a pair of deflection plates and is incident upon a planar screen mounted perpendicular to the axis of the undeflected beam. The undeflected beam is adjusted for best focus on the screen, and in this condition it is incident over a small circular region on the screen. When the beam is deflected, the spot on the screen becomes oval in shape and of area larger than that produced by the undeflected beam. Four rays, which are initially at the outer edge of the beam, are shown in the figure. Ray 1 is closest to the positive deflection plate when the beam passes between the plates, and ray 2 is closest to the negative deflection plate. Rays 3 and 4 are at the sides of the beam. Clearly, electrons in the upper part of the beam are in a region of higher potential as they pass between the plates, and they will remain in the deflecting field

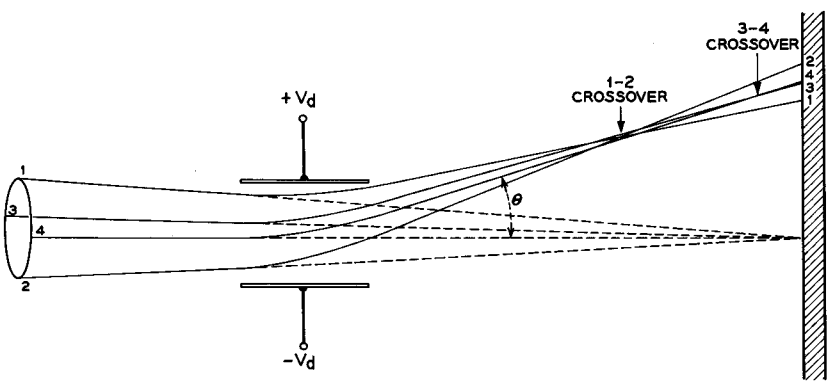

FIG. 3.3-3 The deflection defocusing effect.

for a shorter time than those in the lower part of the beam. Consequently, electrons in the upper part of the beam will be deflected less than those in the lower part of the beam, and rays 1 and 2 will cross at a point well in front of the screen. Rays 3 and 4 cross over somewhat closer to the screen but still in front of it, since the distance to the screen is further when the beam is deflected. The effect of the deflecting field in causing rays 1 and 2 to cross over sooner than rays 3 and 4 is called *deflection defocusing*. For a given mean angle of deflection and a given beam diameter, the difference between the deflection of rays 1 and 2 decreases as the length of the deflection plates increases. In applications where small deflection defocusing is particularly desirable, relatively long deflection plates are used.

Magnetic deflecting fields also cause defocusing effects similar to those illustrated in Figure 3.3-3. However, since the electrons maintain a constant velocity in passing through a magnetic deflecting field, the deflection defocusing for a given angle of deflection is less in a magnetic deflecting field than in an electrostatic deflecting field. When large deflection angles are needed, magnetic deflecting fields are usually employed. Thus in television tubes where the deflection angle (indicated by the angle θ in Figure 3.3-3) may range as high as 55 degrees, only magnetic deflection will give adequate focus of the beam over the whole screen.

In cathode-ray tubes the deflection angles are usually much smaller than in television tubes, generally less than 15 degrees, and the defocusing resulting from electrostatic deflection is usually not severe. Electrostatic deflection is preferred in cathode-ray tubes for two reasons: (1) Electrostatic deflection requires less driving power,[6] and (2) better linearity between beam deflection and the applied deflection signal can be achieved with electrostatic deflection.

3.4 The Spreading of an Electron Beam Because of Its Own Radial Electric Field; Focusing and Confining Beams by Applied Axial Fields

In a number of microwave tubes it is desirable to use a small-diameter electron beam with high axial charge density. Such a beam generates a

---

[6]To illustrate this point, consider the energy per unit volume which must be stored in an electric field and a magnetic field in order to produce a given amount of deflection. If the deflecting force resulting from a magnetic field B is equal to that from an electric field E, then $Beu = eE$, and $Bu = E$. The ratio of the energy stored per unit volume in the magnetic field to that stored in the electric field is $(B^2/2\mu_o)/(\varepsilon_o E^2/2) = B^2c^2/E^2 = c^2/u^2$, where c is the velocity of light, and where use has been made of the relations $\mu_o\varepsilon_o = 1/c^2$ and $Bu = E$. Since c is always greater than u, more energy per unit volume must be stored in the magnetic field in order to produce a given amount of deflection. Furthermore, the deflecting coils are generally outside the tube so that the volume in which the energy is stored is appreciably greater with magnetic deflection. These two factors combine to require much higher driving powers in the case of magnetic deflection than with electrostatic deflection.

radial electric field, which in the absence of other applied fields causes the beam to spread, the off-axis electrons being deflected away from the axis. Usually it is desirable to prevent the beam from spreading, and this can be accomplished in several ways: (1) By directing the beam into a region of uniform axial magnetic field of sufficient intensity, (2) by directing the beam along the axis of a series of equally spaced magnetic or electric lenses of suitable strength, or (3) by directing the beam along the axis of a bifilar helix with the two windings at different potentials. We shall first describe the spreading of an electron beam because of its radial electric field. Later we shall consider the use of axial magnetic and electric fields to prevent the beam from spreading.

The axial linear charge density of a beam of current I_o amperes and electron velocity u_z meters per second is I_o/u_z coulombs per meter. From Equation (1.4-5) the radial electric field intensity at the surface of the beam is

$$E_r = -\frac{I_o}{2\pi\varepsilon_o r u_z} \tag{3.4-1}$$

where r is the beam radius. For a beam current of 10 ma, a beam diameter of 1 mm, and a beam voltage[7] of 1000 volts, Equation (3.4-1) indicates a radial electric field intensity at the surface of the beam of 19 kv/meter, or 19 volts/mm.

If the beam in the above example passed concentrically within a conducting cylinder of inside diameter 2 mm, the potential at the surface of the beam would be 6.6 volts less than that of the cylinder; and if the charge density across the beam were uniform, the potential at the center of the beam would be 11.4 volts less than that of the cylinder. However, in practice, the beam generates positive ions as a result of collisions between the electrons in the beam and molecules of residual gas in the tube. Since the radial field of the beam acts on the ions with a force directed toward the axis, the ions are entrapped by the beam. (The kinetic energy of the ions at the time they are generated is usually a small fraction of an electron volt, and this is not sufficient to overcome the potentials resulting from the radial field of the beam.) The trapping of ions by the beam in turn reduces the net axial charge density and thereby reduces the radial electric field. Generally, the ions tend to "drain" in the axial direction, since in most cases there is a region of lower potential at at least one end of the beam. The extent to which the beam charge is neutralized is therefore determined in part by the potential gradients along the axis of the beam and in part by the residual gas pressure within the tube.

Hines *et al.*[8] describe experimental measurements of the ion neutralization

[7]The net voltage through which the electrons have been accelerated.
[8]Reference 3.6.

of a beam having a current of 14.5 ma, a length of 17 cm, and a beam voltage of 950 volts. An axial magnetic field of 0.075 weber/meter^2 (750 gauss) was used to focus the beam. (See later in this section for focusing with magnetic fields.) The ions drained toward one end of the beam only, the potential at the other end being higher than that of the main portion of the beam. It was concluded that the beam was about 14 per cent neutralized with ions at a tube pressure of 10^{-7} mm of Hg, 50 per cent neutralized at a tube pressure of 10^{-6} mm of Hg, and nearly fully neutralized at a pressure of a few times 10^{-6} mm of Hg. Pressures of the order of 10^{-7} to 10^{-5} mm of Hg might be typical of those attained in a beam-type microwave tube.

If there is no neutralization of the electron space charge by ions, the radial motion of the electrons at the outer edge of the beam as a result of the radial electric field intensity is described by the equation

$$m\frac{d^2r}{dt^2} = mu_z^2\frac{d^2r}{dz^2} = -eE_r = \frac{eI_o}{2\pi\epsilon_o r u_z} \tag{3.4-2}$$

If u_z is constant, this equation can be solved with the aid of tabulated functions.[9] The results are plotted in Figure 3.4-1 for the case of a beam in

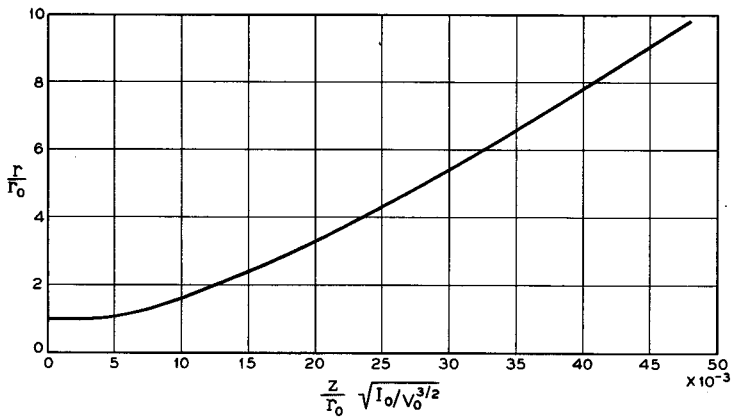

FIG. 3.4-1 The universal beam spread curve.

which the electron trajectories are assumed to be initially parallel to the axis. The plot shows the radius r of the beam as a function of distance z along the beam, the initial radius being r_o. The curve is sometimes called the universal beam spread curve. If the current density over the beam cross section is initially uniform, the radial field will deflect the trajectories

[9]Reference 3.7, p. 443.

of electrons in the interior of the beam by an amount proportional to their initial distance from the axis, and at points further along the beam, the current density over the beam cross section will still be uniform.

For a 10-ma, 1000-volt beam of initial diameter 1 mm in which the trajectories are parallel to the axis at $z = 0$ and in which no ion neutralization takes place, the beam diameter would be 1.8 mm one centimeter further along the axis and 9 mm four centimeters along the axis. With partial ion neutralization the spreading would be less.

In traveling-wave tubes the electron beam must travel inside a long cylindrical region defined by the slow-wave circuit of the tube with essentially no interception of the beam by the slow-wave circuit. Often the slow-wave circuit consists of a wire helix of length perhaps 70 to 250 times its inside diameter. For the beam to travel inside such a slow-wave circuit, additional fields must be applied to prevent the beam from spreading. Several methods for doing this, involving the use of axial electric or magnetic fields, are considered under separate headings below.[10]

(a) *A Uniform Axial Magnetic Field*

Figure 3.4-2 shows a magnetic circuit which produces a long region of uniform magnetic field parallel to its axis. An electron gun is located within the left-hand pole piece and, because the pole piece acts as a magnetic shield, there is essentially zero magnetic field in the region of the gun. We shall assume that the transition along the axis from the region of zero magnetic field to the full magnetic field takes place over a very short axial distance. Suppose a single electron approaches the transition region from the side of zero magnetic field along a path which is initially parallel to the axis but displaced a distance r_o from it. In passing through the transition region the electron acquires an angular velocity about the axis, which from Equation (3.2-6) is given by

$$\dot{\theta} = \frac{\eta B_z}{2} \tag{3.4-3}$$

[10]At first thought it might seem that the beam diameter could be adequately limited by establishing a high enough gas pressure in the tube that the electron charge would be almost fully neutralized by ion charge. However, there would always be a small excess of electrons in the beam and hence a small radial field, since otherwise the ions would be free to escape. This small radial field would cause too much spreading of the beam for most traveling-wave tube applications. Furthermore, higher gas pressures result in greater ion bombardment of the cathode and shorter cathode life. High ion densities also result in mechanical oscillation of large numbers of the ions within the potential well formed by the electron beam. The ion motion modulates the beam and thereby causes a type of noise, called ion oscillation noise, to appear in the output of the tube.

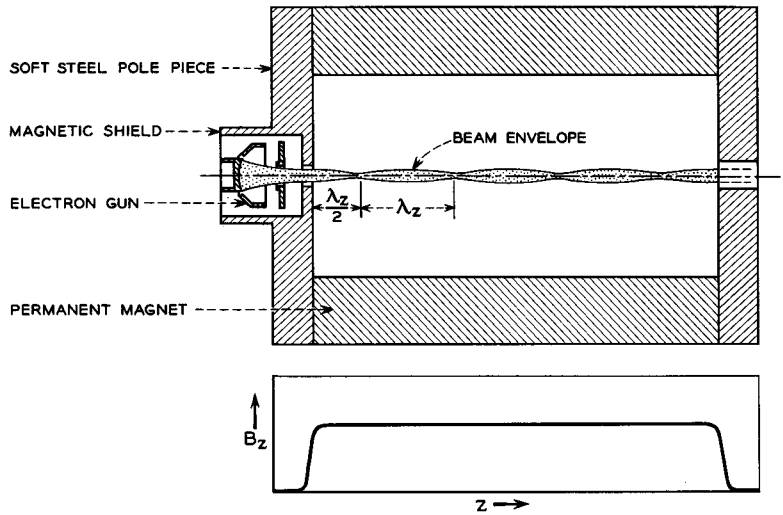

FIG. 3.4-2 An electron beam directed into a region of uniform magnetic field

where B_z is the uniform axial magnetic field, and $\eta = e/m$. If the electron passes through the transition region sufficiently quickly, it will still be at distance r_o from the axis upon entering the region of uniform axial field. Its velocity in the θ direction therefore will be

$$u_\theta = r_o\dot{\theta} = r_o\frac{\eta B_z}{2} \tag{3.4-4}$$

This transverse velocity causes the electron to cross the lines of axial magnetic field, so that the motion of the electron in the transverse plane is circular with radius

$$r = \frac{u_\theta}{\eta B_z} = \frac{r_o}{2} \tag{3.4-5}$$

The electron therefore travels through the uniform magnetic field in a helical path of radius $r_o/2$, and since it initially started at distance r_o from the axis, with velocity only in the θ and z directions, it periodically passes through the axis and returns to its original radius r_o. Interestingly enough, this result is independent of the magnitude of the axial magnetic field, the initial electron velocity, or the initial distance of the electron from the axis. The time taken for the electron to complete one turn of its helical path is $\pi r_o/u_\theta$, so that the points at which the electron passes through the axis are separated by an axial distance given by

$$\lambda_z = u_z\frac{\pi r_o}{u_\theta} = u_z\frac{2\pi}{\eta B_z} \tag{3.4-6}$$

Suppose a cylindrical electron beam of very low axial charge density is directed along the axis of the magnetic circuit shown in Figure 3.4-2. We shall assume that the axial charge density is sufficiently small that the radial electric field of the beam exerts a much weaker transverse force on the off-

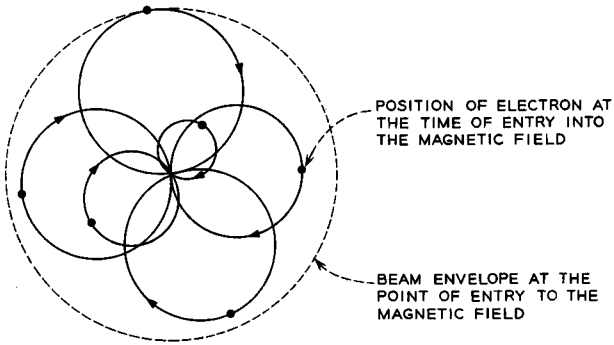

FIG. 3.4-3 The broken line shows the beam envelope at the time the beam is launched into the magnetic field. The motion of individual electrons in the transverse plane after entering the magnetic field is shown by the solid lines.

axis electrons than the force exerted by the magnetic field. In such a beam, electrons which travel along paths that are parallel to the axis just before entering the magnetic field follow helical paths in the region of uniform magnetic field with one side of the helical path touching the axis. Each electron passes through the axis at points spaced by a distance λ_z, the first point being $\lambda_z/2$ beyond its point of entry into the magnetic field. Figure 3.4-3 shows the motion of the electrons in the transverse plane. Since all the electrons pass through (or close to) the axis at nearly the same points, the beam envelope necks down from its initial radius to a very small radius at a point $\lambda_z/2$ beyond the point of entry into the magnetic field and each λ_z thereafter. The beam envelope therefore resembles that shown in Figure 3.4-2 and is said to be "scalloped." For a 1000-volt beam and $B_z = 0.05$ weber/meter^2, $\lambda_z = 1.3$ cm.

Since electrons that enter the magnetic field with large r_o have greater kinetic energy in the transverse plane than those that enter with small r_o and since all electrons in the beam have essentially the same total kinetic energy, the outer electrons will have slightly smaller axial velocity in the region of uniform magnetic field. The total kinetic energy of an electron in the region of uniform magnetic field can be expressed as

$$eV_o = \tfrac{1}{2}m(u_\theta^2 + u_z^2) = \tfrac{1}{2}m[(r_o\eta B_z/2)^2 + u_z^2] \qquad (3.4\text{-}7)$$

where V_o is the voltage through which the electrons have been accelerated. Clearly, an electron that enters the magnetic field with large r_o will have smaller u_z, and hence smaller λ_z, in the region of uniform magnetic field than one that enters with small r_o. Consequently, the outer electrons in the beam will gradually slip behind the inner electrons, and the envelope will be only quasi-periodic in the axial direction.

As the axial charge density of the beam is increased, so that the transverse force from the radial electric field becomes comparable with that resulting from the axial magnetic field, the electron motion is appreciably modified. Brillouin[11] has described an exact solution for electron flow in an axial magnetic field in which the outward force resulting from the radial electric field of the beam is balanced by the inward force of the axial magnetic field. The conditions required for Brillouin flow are difficult to achieve in practice, but the solution defines a value of magnetic flux density in terms of the beam current, the beam voltage, and the beam diameter, and it is often helpful to measure the field actually needed to confine a beam to a given diameter in terms of this field.

To obtain Brillouin flow, the following conditions must apply at the point of entry of the beam to the region of uniform magnetic field:

1. The beam must have a uniform current density across its diameter.
2. The electron trajectories must be parallel to the axis just before entering the magnetic field.
3. The transition from zero axial magnetic field to the full field must occur over a very short axial distance.
4. The beam axis must coincide with that of the magnetic field.

In addition, there must be no trapping of ions by the electron beam.

In Brillouin flow an electron which enters the magnetic field at distance r_o from the axis experiences a radial force which is just sufficient to keep it moving in a helical path of radius r_o about the axis of the beam. The transverse force of the magnetic field must then be sufficient to account for the radial acceleration of the electron when moving in a helical path of radius r_o plus the force resulting from the radial electric field at radius r_o. The axial magnetic field is therefore determined by the relation

$$B_z e u_\theta = \frac{m u_\theta^2}{r_o} - e E_{r_o} \tag{3.4-8}$$

If the beam radius is a and if the current density is uniform across the beam cross section, we can use Equation (3.4-1) to express the second term on the

---

[11]Reference 3.8.

right as

$$eE_{r_o} = -\frac{r_o^2}{a^2}\frac{eI_o}{2\pi\varepsilon_o r_o u_z} = -\frac{r_o}{a^2}\frac{eI_o}{2\pi\varepsilon_o(2\eta V_o)^{1/2}} \tag{3.4-9}$$

where V_o is the voltage through which the electrons have been accelerated. Combining Equations (3.4-4), (3.4-8), and (3.4-9), we obtain

$$B_z^2 = \frac{\sqrt{2}\, I_o}{\pi\varepsilon_o\eta^{3/2}V_o^{1/2}a^2} = \frac{0.69 \times 10^{-6}I_o}{V_o^{1/2}a^2} \tag{3.4-10}$$

This equation gives the magnetic flux density required for Brillouin flow. Since it is independent of the radius r_o, the same magnetic field applies to all electron trajectories for which $r_o \leq a$. For a 10-ma, 1000-volt beam of diameter 1 mm, the Brillouin magnetic flux density is 2.95×10^{-2}weber/meter^2, or 295 gauss.

In Brillouin flow the beam envelope maintains a constant diameter through the region of longitudinal magnetic field, the individual electrons following helical trajectories which are concentric with the beam axis, and the beam as a whole twisting about its axis with angular velocity $\dot{\theta} = \eta B_z/2$. In a thin "cross-sectional slab" of the beam the individual electrons maintain their positions relative to each other, and the slab as a whole rotates about the axis with angular velocity $\dot{\theta}$.

However, in practice, the axial charge density of the beam will be partially neutralized with ions. In this case the transverse force resulting from a magnetic field equal to the Brillouin field would predominate, so that the electrons would periodically pass near to the axis, and the beam envelope would be scalloped. Furthermore, most convergent electron guns[12] give rise to sufficiently high transverse velocities that the maxima in the diameter of the scallops would be somewhat larger than the beam diameter at the point of entry into the magnetic field. (This point is further discussed in Reference 3g.) However, it is found that by increasing the magnetic field, the maximum diameter of the scallops can be reduced. Often a magnetic field equal to $1\frac{1}{2}$ to 3 times the Brillouin field is used.

As the magnetic field is increased appreciably above the Brillouin value, the transverse force resulting from the magnetic field becomes the principal transverse force acting on the electrons. Harker[13] and Ashkin[14] have concluded on the basis of experimental measurements that with a magnetic field greater than, or equal to, about three times the Brillouin field, the effects of the radial electric field can be neglected, and a majority of the

---

[12]Guns which generate a beam of smaller diameter than that of the cathode.
[13]Reference 3.10.
[14]Reference 3.11.

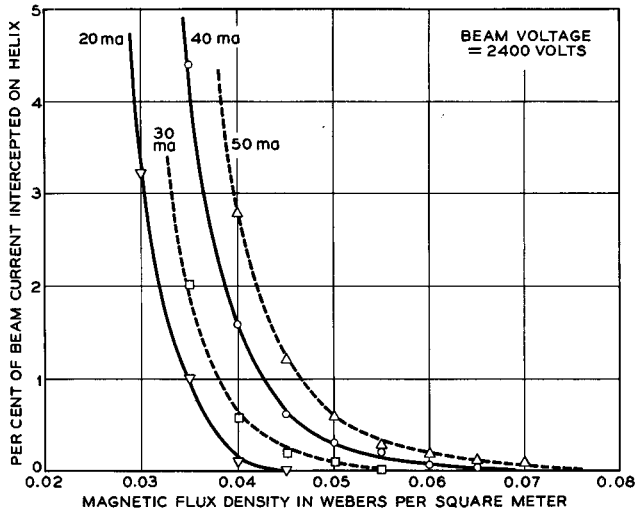

FIG. 3.4-4 Measurements of the beam interception by the slow-wave circuit of a traveling-wave amplifier as a function of the applied axial magnetic flux density. The beam was generated by the electron gun illustrated in Figure 4.5-1(a). (From J. P. Laico *et al.*, *Bell System Tech. J.* **35**, 1285, 1956. Reprinted by permission of American Telephone and Telegraph Company)

electrons pass through, or very close to, the beam axis. In this case an electron that enters the magnetic field at distance r_o from the axis travels in a nearly helical path of radius $r_o/2$ and periodically passes through or close to the axis.

Figure 3.4-4 shows measurements of the fraction of the beam current intercepted on a helix-type slow-wave circuit of a traveling-wave amplifier as a function of the applied axial magnetic flux density. The data are plotted for several values of beam current. The helix had an inside radius of 1 mm and a length of 17 cm. The electron gun was similar to that shown in Figure 4.5-1(a). A plot of current density vs. radius for the electron beam at the point of entry into the magnetic field is shown in Figure 4.5-4. An electron emitted from the edge of the cathode with zero emission velocity in the direction parallel to the cathode surface arrives at the point of entry into the magnetic field at a radius of 0.45 mm from the beam axis. However other electrons emitted from the edge of the cathode with relatively high emission velocity parallel to the cathode surface arrive at the point of entry into the magnetic field at distances from the beam axis as high as 0.7 to 0.8 mm.

Figure 3.4-4 shows that with increasing beam current, a higher magnetic field was required to prevent interception of the beam by the helix, as would

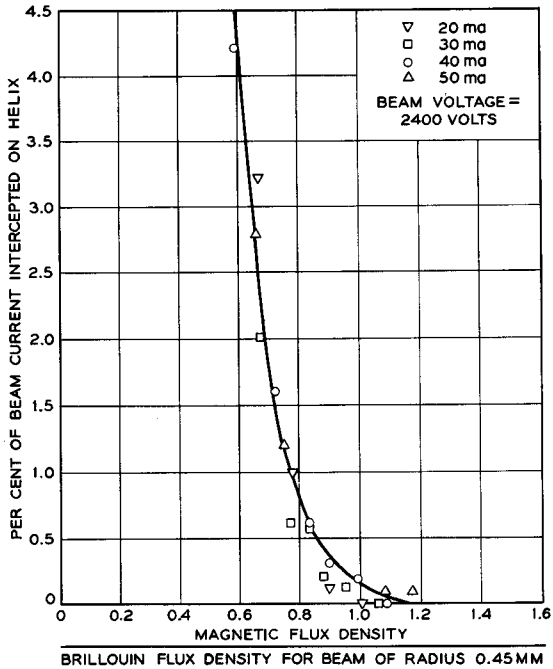

FIG. 3.4-5 The data for Figure 3.4-4 are plotted vs. the ratio of the actual magnetic flux density to the Brillouin flux density for a beam of uniform current density and a radius of 0.45 mm.

be expected from Equation (3.4-10). Figure 3.4-5 shows the same data plotted as a function of the ratio of the actual magnetic flux density to the Brillouin flux density for a beam of uniform current density and radius 0.45 mm.

(*b*) *Confined Flow*[15]

A type of electron flow, known as confined flow, is achieved with the electron gun entirely immersed in the magnetic field. Often a uniform axial magnetic field is used. The cathode of the electron gun might consist of a planar disc which is perpendicular to the field, whereas the accelerating electrode would have an aperture somewhat larger than the cathode diameter. An electron gun that is used with confined flow (and has several accelerating electrodes) is illustrated subsequently in Figure 4.5-1(c).

[15]Reference 3b, p. 161.

If the magnetic field lines are parallel to the beam axis over the entire length of the beam, starting at the cathode, the beam diameter obtained with confined flow is always larger than the cathode diameter, but it decreases and asymptotically approaches the cathode diameter as the magnetic field intensity is increased. With increasing magnetic field the electrons increasingly tend to follow the field lines, and the motion of an individual electron in the transverse plane becomes limited to a smaller and smaller area, the motion being nearly circular.

With confined flow the magnetic field required to confine a given beam current to a given diameter is always greater than that needed when the beam is generated outside the magnetic field and injected into it, as described in Section (a) above. Confined flow has found its chief application in low-noise microwave amplifier tubes, where the magnetic field in the region of the potential minimum reduces the transverse motion of the electrons and thereby effects a reduction in the noise generated by the beam.

Confined flow also can be achieved with a convergent electron gun by establishing in the region of the gun a magnetic field that converges in the same manner as the electron trajectories in the absence of the magnetic field. In this case the electrons "follow the magnetic field lines" through the accelerating region of the gun, and in the region beyond the gun their motion is much as described above.

(c) *Focusing with Periodic Magnetic Fields*

A series of equally spaced lenses also can be used to focus an electron beam. In this case the off-axis electrons experience a radial impulse, which is directed toward the axis, as they pass each lens. The impulses deflect the electrons toward the axis, but between lenses the beam again spreads because of the radial electric field due to the space charge. For a particular condition of lens strength and spacing and for a particular average beam radius, the impulses from the lenses just balance the integrated radial outward force resulting from the space charge of the beam, and the beam diameter at successive lenses remains constant. The shape of the beam envelope is then somewhat as illustrated in Figure 3.4-6. Focusing an electron beam

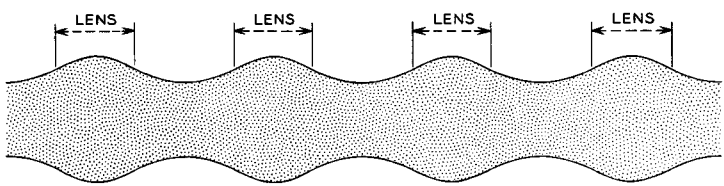

FIG. 3.4-6 The focusing action of a series of equally spaced lenses.

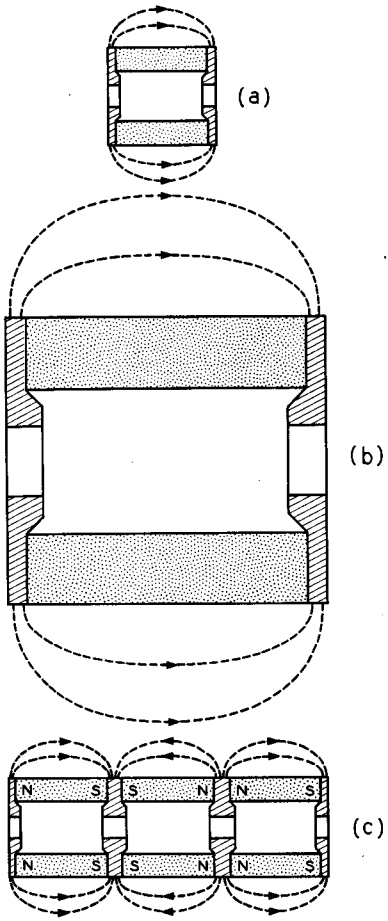

FIG. 3.4-7 The use of a periodic focusing structure reduces the weight of magnetic material needed to produce a given magnetic field over a given axial distance. (From J. T. Mendel *et al.*, *Proc. IRE* **42**, 800, 1954)

with a series of equally spaced lenses is called periodic focusing, since the axial field varies periodically in the z direction.

The stability of periodic focusing can be made plausible by noting that if the beam radius increases above that needed to obtain the balance condition, the radial impulses received from the lenses predominate, and the off-axis electrons receive a net deflection toward the axis. On the other hand, if the beam radius becomes less than that required for balance, the radial outward force predominates and the beam expands.

Periodic focusing can be achieved with both electric lenses and magnetic lenses. When magnetic lenses are used, the axial fields of successive lenses are usually reversed in direction, and in this way a substantial reduction in magnet weight can be achieved over that of a permanent magnet or electromagnet which would produce a uniform axial focusing field.[16] To explain this, we might first note that the magnetic circuit shown in Figure 3.4-2 establishes a magnetic field throughout a far larger volume than that occupied by the beam, and, since the total weight of the magnet material is closely related to the magnetic energy stored in the space surrounding the magnet, much of the weight of the magnet would appear to be wasted.

Figure 3.4-7 illustrates how weight can be saved using a periodic permanent magnet circuit. The magnetic circuit shown in Figure 3.4-7(a) is assumed to produce a uniform axial magnetic field over the length of the

[16]Reference 3.12.

magnet. By increasing all the linear dimensions of the circuit by a factor of 3, as in the magnetic circuit shown in part (b) of the figure, the length of the axial magnetic field is increased by three times, but the magnitude of the axial field remains unchanged. The larger magnet weighs $3^3 = 27$ times as much as the smaller magnet, and the energy stored in the space surrounding it is 27 times as great. On the other hand, three of the smaller magnets placed end for end with like poles together (i.e., north beside north and south beside south), as in the assembly shown in Figure 3.4-7(c), have 1/9 the weight of the larger magnet and produce approximately the same axial field over the same axial distance, but with two reversals in direction. The energy stored in the space surrounding the three magnets in Figure 3.4-7(c) is approximately 1/9 that stored in the space around the larger magnet, since the leakage fields extend only 1/3 as far from the axis.

If the larger magnet were replaced with n smaller permanent magnets of the same total overall length and axial magnetic field, the weight of the periodic circuit would be $1/n^2$ times that of the larger magnet. However, in practice the reversals of the axial field are not really abrupt and, in order to achieve adequate focusing of the beam, a somewhat higher peak magnetic field must be used. This requires the magnets of the periodic structure to be somewhat heavier, and consequently the weight of the periodic circuit needed to focus a given beam is between $1/n^2$ and $1/n$ that of a single permanent magnet which would focus the beam with a uniform axial field.

Periodic structures also have the advantage of much smaller leakage fields and hence less likelihood of interference with nearby devices or equipment.

Let us now examine the electron motion in a periodic magnetic field. Equations (3.1-4) and (3.2-8) can be combined to give an equation that describes the radial motion of an electron in the presence of both an axial magnetic field and a radial electric field, namely

$$\frac{d^2r}{dt^2} + \left(\frac{\eta B_z}{2}\right)^2 r - \eta \frac{dV}{dr} = 0 \tag{3.4-11}$$

Suppose the axial magnetic field varies as a cosine function, so that

$$B_z = B_o \cos \frac{2\pi z}{L} \tag{3.4-12}$$

where L is the magnet period, or twice the center-to-center distance between adjacent pole pieces. Substituting for $dV/dr = -E_r$ from Equation (3.4-1), setting $z = u_z t$, and combining Equations (3.4-11) and (3.4-12), we obtain the following equation for the motion of an electron at the surface of the beam:

$$\frac{d^2r}{dz^2} + \left(\frac{\eta B_o}{2u_z} \cos \frac{2\pi z}{L}\right)^2 r - \frac{\eta I_o}{2\pi\varepsilon_o u_z^3} \frac{1}{r} = 0 \tag{3.4-13}$$

It is convenient to make a change of variables and rewrite this equation in the form

$$\frac{d^2\sigma}{dT^2} + \alpha(1 + \cos 2T)\sigma - \frac{\beta}{\sigma} = 0 \tag{3.4-14}$$

where

$$\sigma = \frac{r}{a}, \qquad T = \frac{2\pi z}{L}$$

$$\alpha = \frac{1}{2}\left(\frac{\eta B_o L}{4\pi u_z}\right)^2 = 2.79 \times 10^8 \frac{B_o^2 L^2}{V_o}$$

$$\beta = \frac{\eta I_o L^2}{8\varepsilon_o \pi^3 u_z^3 a^2} = \frac{385 I_o L^2}{V_o^{3/2} a^2}$$

and where use has been made of the relations $u_z^2 = 2\eta V_o$ and $2\cos^2 T = 1$

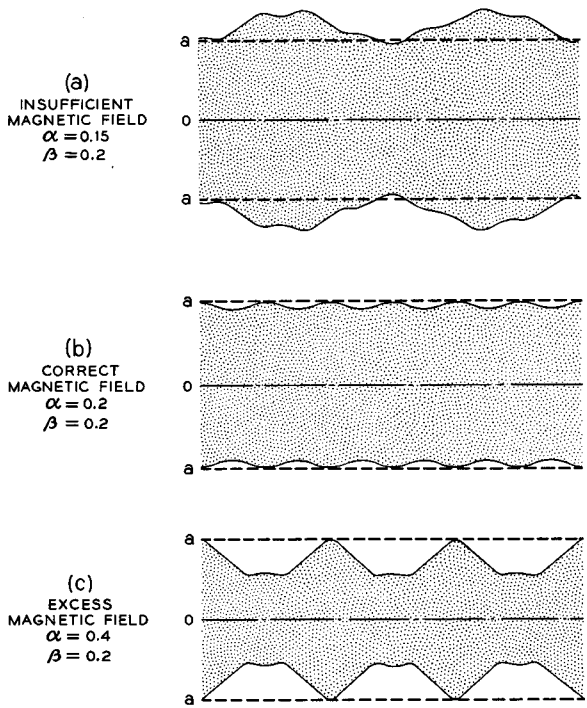

FIG. 3.4-8 The shape of the envelope of a beam for three conditions of the magnetic field parameter α. The small ripples on the beam are associated with the pole piece spacing $L/2$. (From J. T. Mendel *et al.*, *Proc. IRE* **42**, 800, 1954)

$+ \cos 2T$. The beam radius at the point of entry into the magnetic field is assumed to be a.

Solutions to Equation (3.4-14) have been obtained with the aid of an analog computer[17] for the case in which: (1) The electron flow is "laminar," that is, the electron trajectories do not cross one another; and (2) the current density across the beam cross section is uniform. (Also implicit in Equations (3.4-13) and (3.4-14) is the assumption of no ion neutralization.) The shape of the beam envelope as determined by the computer for three values of the axial magnetic field is shown in Figure 3.4-8. The computer results show that minimum beam ripple is obtained when $\alpha = \beta$ or

$$B_{\text{rms}}^2 = 0.69 \times 10^{-6} \frac{I_o}{V_o^{1/2} a^2} \tag{3.4-15}$$

where $B_{\text{rms}} = B_o/\sqrt{2}$. It will be noted that the right-hand side of this equation is the same as that of Equation (3.4-10), which gives the Brillouin field needed to focus a beam of current I_o, voltage V_o, and radius a. Thus for a sinusoidally varying field the rms value of the magnetic field must equal the Brillouin field. This result is perhaps not surprising, since the radial force resulting from the axial magnetic field is proportional to B_z^2, and with a sinusoidal field such that $B_{\text{rms}} = B_{\text{Brillouin}}$, the average radial force from the magnetic field is the same as with Brillouin flow.

By setting $\beta = 0$ in Equation (3.4-14), the equation reduces to a form of Mathieu Equation[18] that is characterized by solutions for σ which are periodic in T for certain ranges of α, and which are unstable for other ranges of α. Figure 3.4-9 shows the ranges of α for which the solutions are stable.

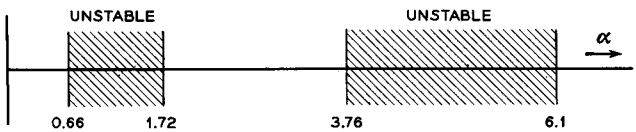

FIG. 3.4-9 The regions in which Equation (3.4-14) is unstable when $\beta = 0$.

The significance of this is that, if we reduce the beam current I_o to a vanishingly small value, so that $\beta \to 0$, but maintain constant beam voltage, there will be some values of the parameters B_o, L, and V_o for which the beam will be focused by the lenses and others for which $\sigma = r/a$ will be unstable and the beam will become divergent. Furthermore, it is found[19] that even with higher beam currents the periodic structure transmits practically no current in the regions marked "unstable" in Figure 3.4-9.

---

[17]Reference 3.13.
[18]Reference 3.14.
[19]Reference 3.13.

In practice, most periodic circuits are designed to operate in the first "pass band" in Figure 3.4-9, corresponding to $\alpha < 0.66$. To determine the value of B_o that should be used, the beam is first focused with a solenoid which produces a uniform axial field, and the minimum value of B_z which gives good beam transmission is measured. The value of B_o for the periodic circuit is then taken to be approximately $\sqrt{2}$ times this field (assuming that the axial field is to vary in a nearly sinusoidal manner). The period L of the periodic circuit is then determined so that α is less than 0.66, perhaps 30 per cent less. For $B_o = 0.08$ weber/meter^2 (or 800 gauss), and a beam voltage of 1500 volts, a period L of 1.92 cm gives an α of 0.44. Reference 3.15 describes the design of the pole pieces and permanent magnets for a periodic circuit.

(*d*) *Periodic Focusing with Electric Fields*

Tien[20] has described the focusing of an electron beam using a periodic electric field. Such a field might be obtained with a series of ring electrodes as illustrated in Figure 3.4-10(a) or a bifilar helix such as that illustrated in Figure 3.4-10(b). In both cases the outer electrons experience a relatively strong force toward the axis when they are close to the electrodes at the

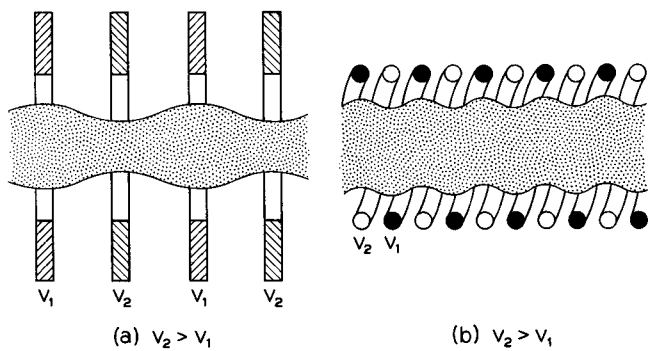

FIG. 3.4-10 Periodic focusing of a beam with electric fields: (a) with a series of ring electrodes, and (b) with a bifilar helix.

lower potential and a somewhat weaker outward force when they are opposite the electrodes at the higher potential. Also, their axial velocity is less when they experience the inward force than when they experience the outward force. Consequently, there is a net focusing effect that can be used to balance the outward force of the radial electric field of the beam. As in the case of periodic focusing with magnetic fields, the beam radius is

[20]Reference 3.16.

found to be stable for some values of the focusing parameters, whereas for others it becomes divergent.

Tien pointed out that the bifilar helix also can be used as the slow-wave circuit of a traveling-wave amplifier. Such a tube has been developed by RCA.[21] The helix structure of the RCA tube is illustrated in Figure 3.4-11. The length of the helix is 22 cm. Figure 3.4-12 shows measurements of the per cent beam current intercepted by the helix as a function of the voltages applied to the helix. It can be seen that good focusing is achieved over a range of helix voltages.

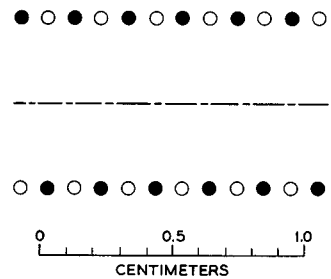

FIG. 3.4-11 The bifilar helix used in an electrostatically focused traveling-wave amplifier developed by RCA. (Courtesy Radio Corporation of America)

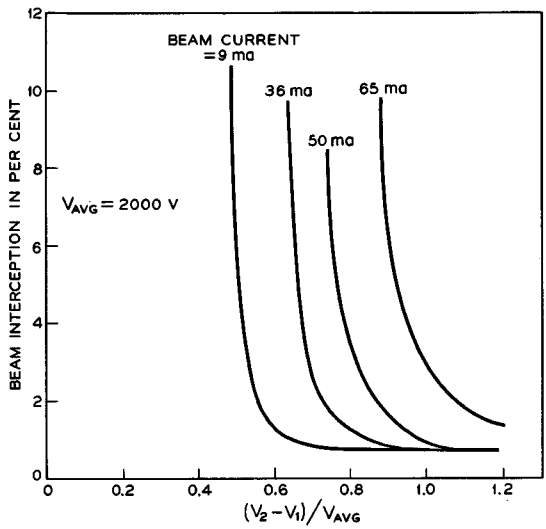

FIG. 3.4-12 Beam interception on the helix structure illustrated in Figure 3.4-11 vs. $(V_2 - V_1)/V_{avg}$, where V_1 and V_2 are the voltages applied to the two helices and $V_{avg} = (V_1 + V_2)/2$. (From D. J. Blattner and F. E. Vaccaro, *Electronics* **32,** No. 1, 46, 1959. Copyright by *Electronics*, a McGraw-Hill Publication)

[21]Reference 3.17.

PROBLEMS

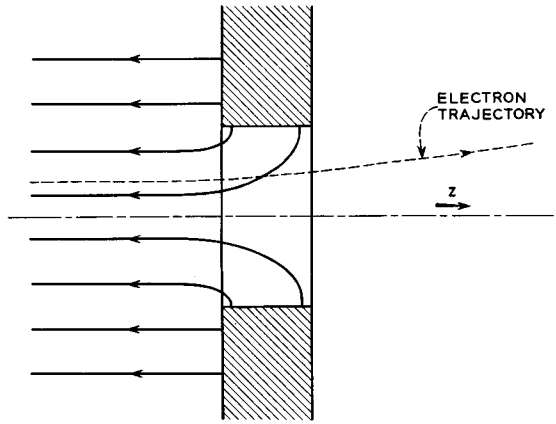

Problem 3.1

3.1 The figure shows an electrode with a small aperture in it. To the left of the electrode there is a uniform potential gradient E_z. An electron approaches the aperture from the left along a path parallel to the axis of the aperture but displaced a small distance from it. As the electron passes through the aperture, the diverging field deflects it away from the axis. Show that the field in the region of the aperture acts as a diverging lens with focal length approximately equal to $4V_o/E_z$, where V_o is the potential through which the electron has been accelerated at the time it passes through the aperture. Assume that the electron's velocity is sufficiently large when it reaches the aperture that the electron remains at nearly constant distance from the axis as it passes through the aperture, and the effect of the radial field is to give the electron an outward impulse.

3.2 A single turn of wire which conducts a current I_o generates an axially symmetric field which can be used as a magnetic lens. Using the expression given in Equation (3.2-13) for the focal length of a weak lens, show that

$$f = \frac{256V_oR}{3\pi\eta\mu_o^2 I_o^2} \approx \frac{98V_oR}{I_o^2}$$

for such a lens, where R is the radius of the turn, and V_o is the beam voltage.

3.3 Sketch a magnetic lens that produces no net rotation of the beam.

3.4 Figure 3.3-3 shows a cylindrical beam of electrons that passes between two parallel deflection plates and is deflected through a mean angle θ. However, because of deflection defocusing effects, electrons at the upper side of the beam are deflected through a slightly smaller angle, which we shall assume to be $\theta - \Delta\theta$, and electrons at the lower side of the beam are deflected through an angle $\theta + \Delta\theta$. Show that for a given beam diameter and given angle θ, the incremental angle $\Delta\theta$ is inversely proportional to the length of the deflection plates. Assume that the field between the deflection plates is uniform, and that the effects of fringing fields

at the ends of the plates can be neglected. (Actually the fringing field at the exit end of the deflecting plates has the effect of reducing the deflection defocusing.)

3.5 Two apertured electrodes, one at higher potential than the other, form an electric lens. An electron beam passes through the lens in the direction of increasing potential. The electrode at lower potential has a wire grid across its aperture and is in contact with the grid. The wires of the grid are laid in two directions at right angles so as to produce a fine mesh. Show qualitatively that a beam passing through the lens experiences a *diverging* action. Note that this does not contradict the statements made in section 3.1 about *axially symmetric* fields acting as converging lenses.

3.6 Show that with Brillouin flow all the electrons of the beam have the same axial velocity, equivalent to that produced by an accelerating potential equal to the potential on the beam axis.

REFERENCES

Several general references pertaining to the material covered in this chapter are:

3a. O. Klemperer, *Electron Optics*, 2nd Ed., Cambridge University Press, Cambridge, England, 1953.
3b. J. R. Pierce, *Theory and Design of Electron Beams*, 2nd Ed., D. Van Nostrand Co., Inc., Princeton, N. J., 1954.
3c. V. K. Zworykin, G. A. Morton, E. G. Ramberg, J. Hillier, and A. W. Vance, *Electron Optics and the Electron Microscope*, John Wiley and Sons, Inc., New York, 1945.
3d. V. K. Zworykin and G. A. Morton, *Television*, 2nd Ed., John Wiley, and Sons, Inc., New York, 1945.
3e. K. R. Spangenberg, *Vacuum Tubes*, Chapters 13, 14, 15, McGraw-Hill Book Co., Inc., New York, 1948.
3f. P. Grivet, *Advances in Electronics*, Vol. II, p. 47, 1950.
3g. G. R. Brewer, "Some Characteristics of a Magnetically Focused Electron Beam — Parts I and II, "*Technical Memoranda No. 495* and *No. 528*, Research Laboratories, Hughes Aircraft Co., Culver City, Calif.
3h. P. A. Lindsay, "Velocity Distribution in Electron Streams," *Advances in Electronics and Electron Physics* **XIII**, 182, 1960.

Other references covering specific subjects discussed in Chapter 3 are:

3.1 S. Bertram, *Proc. IRE* **28**, 418, 1940.
3.2 L. S. Goddard, *Proc. Cambridge Phil. Soc.* **42**, 106, 1946.
3.3 K. Spangenberg and L. M. Field, *Proc. IRE* **30**, 138, 1942.
3.4 G. Liebmann, *Advances in Electronics* **II**, 102, 1950.
3.5 K. R. Spangenberg and L. M. Field, *Elec. Comm.* **21**, 194, 1943.
3.6 M. E. Hines, G. W. Hoffman, and J. A. Saloom, *J. Appl. Phys.* **26**, 1157, 1955.
3.7 K. R. Spangenberg, *Vacuum Tubes*, McGraw-Hill Book Co., Inc., 1948.
3.8 L. Brillouin, *Phys. Rev.* **67**, 260, 1945.
3.9 J. P. Laico, H. L. McDowell, and C. R. Moster, *Bell System Tech. J.* **35**, 1285, 1956.
3.10 K. J. Harker, *J. Appl. Phys.* **28**, 645, 1957.
3.11 A. Ashkin, *J. Appl. Phys.* **29**, 1595, 1958.

3.12 J. R. Pierce, *J. Appl. Phys.* **24**, 1247, 1953.
3.13 J. T. Mendel, C. F. Quate, and W. H. Yocom, *Proc. IRE* **42**, 800, 1954.
3.14 N. W. McLachlan, *Theory and Applications of Mathieu Functions*, Oxford University Press, Oxford, England, 1947.
3.15 J. E. Sterrett and H. Heffner, *Trans. IRE* **ED-5**, 35, 1958.
3.16 P. K. Tien, *J. Appl. Phys.* **25**, 1281, 1954.
3.17 D. J. Blattner and F. E. Vaccaro, *Electronics* **32**, No. 1, 46, 1959.